Letter

Degenerate fermionic matter at N^{3}LO: Quantum electrodynamics

Tyler Gorda,[1,2] Aleksi Kurkela,[3] Juuso Österman,[4] Risto Paatelainen,[4] Saga Säppi,[5] Philipp Schicho,[4] Kaapo Seppänen,[4] and Aleksi Vuorinen[4]

[1]*Department of Physics, Technische Universität Darmstadt, 64289 Darmstadt, Germany*
[2]*ExtreMe Matter Institute EMMI and Helmholtz Research Academy for FAIR, GSI Helmholtzzentrum für Schwerionenforschung GmbH, 64291 Darmstadt, Germany*
[3]*Faculty of Science and Technology, University of Stavanger, 4036 Stavanger, Norway*
[4]*Department of Physics and Helsinki Institute of Physics, University of Helsinki, P.O. Box 64, FI-00014 University of Helsinki, Finland*
[5]*European Centre for Theoretical Studies in Nuclear Physics and Related Areas (ECT*) and Fondazione Bruno Kessler, Strada delle Tabarelle 286, I-38123 Villazzano (TN), Italy*

(Received 23 May 2022; accepted 7 December 2022; published 15 February 2023)

We determine the pressure of a cold and dense electron gas to a nearly complete next-to-next-to-next-to-leading order (N^{3}LO) in the fine-structure constant α_e, utilizing a new result for the two-loop photon self-energy from a companion paper. Our result contains all infrared-sensitive contributions to the pressure at this order, including the coefficient of the $O(\alpha_e^3 \ln \alpha_e)$ term, and leaves only a single coefficient associated with the contributions of unresummed hard momenta undetermined. Moreover, we explicitly demonstrate the complete cancellation of infrared divergences according to the effective-field-theory paradigm by determining part of the hard contributions at this order. Our calculation provides the first improvement to a 45-year-old milestone result and demonstrates the feasibility of the corresponding N^{3}LO calculation for cold and dense quark matter.

DOI: 10.1103/PhysRevD.107.L031501

I. INTRODUCTION

The need to quantitatively understand the thermodynamic properties of degenerate fermionic matter is ubiquitous in theoretical physics. Examples of physical systems of interest range from condensed matter physics [1,2] and supersymmetric theories [3,4] to compact astrophysical objects such as white dwarfs [5] and neutron stars [6]. Though the details of these systems vary greatly and the relevant densities and temperatures are separated by orders of magnitude, they all share common features stemming from the Pauli exclusion principle. These properties typically include some type of a filled Fermi sea of hard fermionic excitations with softer bosonic modes mediating their interactions or being formed through pairing on the Fermi surface. While in some cases specific techniques, such as gauge-gravity duality or numerical lattice field theory may offer valuable insights, the only first-principles field-theory tool universally applicable at low temperatures and large chemical potentials is perturbation theory (see e.g., [7] for a recent review). This provides strong impetus to further develop weak-coupling techniques for the study of degenerate fermionic matter.

In the case of ultrarelativistic matter, the foundations of modern perturbative computations were set in the seminal works of Freedman and McLerran in the late 1970s [8–10], where the authors determined the equations of state (EOS) of degenerate quantum electrodynamics (QED) and quantum chromodynamics (QCD) matter to next-to-next-to-leading order (N^{2}LO) in a weak-coupling expansion around a free Fermi gas in powers of the coupling α. At this order, the presence of the two distinct momentum scales in the system becomes tangible: the hard fermionic modes, with momenta of the same magnitude as the chemical potential, $k_F \sim \mu$, can be treated fully perturbatively, while the long-wavelength gauge fields, with momenta proportional to the Debye screening scale $\sqrt{\alpha}\mu$, require a nonperturbative treatment. In [8–10], the soft contributions were accounted for through an explicit resummation of an infinite class of ring diagrams, containing arbitrary numbers of fermionic loops, but at even higher orders such a treatment becomes intractable. Instead, it becomes imperative to treat the physics of the soft momentum scale via an effective-field-theory setup, which has indeed been realized in recent years through the systematic implementation of the hard-thermal-loop (HTL) framework to the description of cold

and dense systems [11–15]. This development has led to several advances, including the unification of perturbative results throughout the temperature-chemical potential plane for deconfined QCD matter [11,15].

For cold and dense quark matter, the first next-to-next-to-next-to-leading order (N^3LO) calculations determined the fully soft contributions to the EOS [13,14], including also the leading logarithmic contribution of $O(\alpha^3 \ln^2 \alpha)$ [12], absent in an Abelian theory. The contributions to the leading and next-to-leading logarithms arising from the fully soft sector have also recently been resummed [16]. However, in order to determine *all* logarithmically enhanced terms at this order, i.e., to reach the $O(\alpha^3 \ln \alpha)$ accuracy, so-called mixed contributions originating from interactions between the hard and soft modes must also be accounted for. In this article, we determine precisely these mixed N^3LO terms for the Abelian theory QED, providing the first improvement to the EOS of this theory since the late 1970s [10,17] (see, however, the related high-temperature calculations [18,19]). This computation serves as a proof of principle of the effective-theory framework and for the first time demonstrates the nontrivial cancellation of divergences arising from the soft and hard sectors at N^3LO, thus paving the way to the conceptually similar but diagrammatically more laborious non-Abelian version of this calculation.

Based on earlier computations within both QED and QCD [10,14,20], we know that up to N^3LO, the pressure p of cold and dense QED matter takes the parametric form [with the leading-order (LO) pressure $p_{\rm LO} = \mu^4 N_f/(12\pi^2)$, μ being the fermion chemical potential, taken here to be equal for each of the N_f flavors]

$$\frac{p}{p_{\rm LO}} = 1 - \frac{3}{2}\left(\frac{\alpha_e}{\pi}\right) - N_f\left(\frac{\alpha_e}{\pi}\right)^2\left[\frac{3}{2}\ln\left(N_f\frac{\alpha_e}{\pi}\right) - \ln\frac{\bar{\Lambda}}{2\mu} - \frac{22}{3} - \frac{51}{8N_f} + \frac{13}{2}\ln 2 + \frac{\pi^2}{2} - 4\ln^2 2 + \frac{3}{4}\delta\right] + N_f^2\left(\frac{\alpha_e}{\pi}\right)^3\left[a_{3,1}\ln^2\left(N_f\frac{\alpha_e}{\pi}\right) + a_{3,2}\ln\left(N_f\frac{\alpha_e}{\pi}\right) + a_{3,3}\ln\left(N_f\frac{\alpha_e}{\pi}\right)\ln\frac{\bar{\Lambda}}{2\mu} + a_{3,4}\ln^2\frac{\bar{\Lambda}}{2\mu} + a_{3,5}\ln\frac{\bar{\Lambda}}{2\mu} + a_{3,6}\right] + O(\alpha_e^4). \tag{1}$$

Here, $\alpha_e(\bar{\Lambda}) = e(\bar{\Lambda})^2/4\pi$ is the renormalized fine-structure constant at the renormalization scale $\bar{\Lambda}$, with e the electric charge of each fermion, also taken to be equal for each of the N_f flavors; while $\delta \approx -0.8563832$ is available via a one-dimensional integral expression that can be evaluated to practically arbitrary precision [20]. The coefficients $a_{3,n}$ are in principle unknown, although $a_{3,3}$–$a_{3,5}$ are available from the lower-order coefficients using the renormalization-scale independence of the pressure (see the Supplemental Material [21]).

The terms we determine in this work include

(i) the full contribution of the purely soft (scale $e\mu$) sector which turns out to identically vanish, implying $a_{3,1} = 0$,
(ii) the full mixed contributions which determine the $a_{3,2}$ coefficient, and
(iii) part of the fully hard contribution, including all of its infrared (IR) divergences and the leading large-N_f part of $a_{3,6}$.

As a result, we are able to explicitly demonstrate the cancellation of all ultraviolet (UV) and IR divergences between the soft and hard sectors at N^3LO, which happens exactly as predicted in [14]. Only one finite coefficient, independent of logarithms and corresponding to the purely hard subleading-in-N_f contributions to $a_{3,6}$, is left missing from the full $O(\alpha_e^3)$ pressure. Our calculation extensively utilizes results from a companion paper [24], where we determine corrections to the one-loop HTL photon self-energy from power corrections in soft momenta and two-loop diagrams, generalizing the results of [25–27] to nonzero μ. Importantly, both calculations pave the way towards completing the same tasks in cold and dense QCD.

II. SETTING UP THE PROBLEM

Following the organizational scheme presented in [14] and translating it to the somewhat simplified case of U(1) gauge symmetry, the N^3LO pressure of cold and dense QED contains contributions from three different kinematic regions. These are dubbed purely soft (s), purely hard (h), and mixed (m), of which the last one couples the soft and hard modes together. As explained in detail in [13], the split between these different kinematic regions is not unique, and this ambiguity renders the individual contributions dependent on an additional factorization scale $\Lambda_{\rm h}$, which must cancel when summing over all contributions at a fixed order (see the beginning of next section for the introduction of $\Lambda_{\rm h}$ in dimensional regularization). We may thus write the N^3LO pressure correction, denoted here by p_3, in the form

$$p_3 = p_3^s + p_3^m + p_3^h, \tag{2}$$

with the three terms on the right-hand side corresponding to the different momentum scales. The first, purely soft contribution arises from interactions among soft, screened photons, which can be described within the HTL effective theory [28]. Due to the vanishing of the photon HTL

N-point function for $N \geq 3$ in QED [29] (and the absence of tree-level gauge interactions), this term vanishes to all orders, so that we immediately obtain the result $p_3^s = 0$.

The mixed and hard pressure terms can, on the other hand, be further split into different subcontributions based on their potential IR sensitivity, as discussed in detail in [14] for QCD. Using a second subscript to denote the number of potential IR divergences in each graph, we obtain

$$p_3^m = p_{3,0}^m + p_{3,1}^m, \tag{3}$$

$$p_3^h = p_{3,0}^h + p_{3,1}^h + p_{3,2}^h. \tag{4}$$

Here, the different terms correspond to the diagrams

$p_{3,0}^m + p_{3,1}^m =$  , (5)

$p_{3,0}^h =$  , (6)

$p_{3,1}^h + p_{3,2}^h =$ 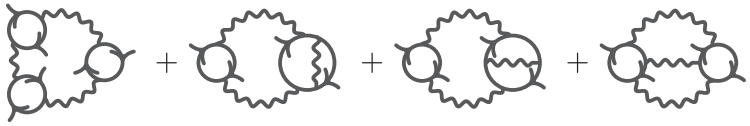 , (7)

where a sum over the direction of fermionic flow is suppressed and HTL-resummed photon lines are denoted by wavy double lines. There are multiple types of divergences present in these diagrams: full-theory (unresummed) UV divergences, full-theory IR divergences and HTL (resummed) UV divergences. Each $p_{3,k}^i$ contains full-theory UV divergences, while full-theory IR divergences are contained within $p_{3,1}^h + p_{3,2}^h$ and the HTL UV divergences are contained within $p_{3,0}^m + p_{3,1}^m$. Note also that the final diagram of Eq. (7) is included in this term only due to its *potential* to be IR sensitive: as explained above, in reality its IR limit is benign in QED, and the term will not produce any real IR divergences.

III. OUTLINE OF THE CALCULATION

We regulate both the UV- and IR-divergent parts of the above diagrams in dimensional regularization in $D = 4 - 2\varepsilon$ dimensions, using the standard modified minimal subtraction scheme ($\overline{\text{MS}}$) measure $[\mathrm{e}^{\gamma_\mathrm{E}}\Lambda^2/(4\pi)]^\varepsilon \mathrm{d}^D K$. It is, however, important to note that two different values are used for the renormalization scale Λ: The full-theory UV divergences are regulated with the standard UV renormalization scale $\bar{\Lambda}$, whereas all the remaining divergences are regulated with the factorization scale Λ_h. The divergences can be unambiguously split in this way due to the specific "ring" structure of the integrals that appear in the expressions, and so we cannot readily generalize this IR-UV split to arbitrary loop integrals.

Concentrating first on the mixed contribution, i.e., Eq. (5) above, we note that the general structure of the UV-renormalized mixed contribution to the QED pressure at N^{3}LO reads

$$p_3^m = \frac{e^2 m_\mathrm{E}^4}{6(4\pi)^4}\left(\frac{m_\mathrm{E}}{\Lambda_\mathrm{h}}\right)^{-2\varepsilon}\left(\frac{p_{-1}^m}{2\varepsilon} + p_0^m\right). \tag{8}$$

Here, $e = e(\bar{\Lambda})$ is the renormalized gauge coupling of QED, while the one-loop electric screening mass at zero temperature but nonzero chemical potential reads $m_\mathrm{E}^2 = N_f e(\bar{\Lambda})^2\mu^2/\pi^2$. This $1/\varepsilon$ divergence remaining after renormalization arises from the separation between the soft and hard momentum scales, hence the appearance of Λ_h in the expression.

Similarly, the general structure of the UV-renormalized hard contribution to the QED pressure at N^{3}LO reads

$$p_3^h = \frac{e^2 m_\mathrm{E}^4}{6(4\pi)^4}\left(\frac{\mu}{\Lambda_\mathrm{h}}\right)^{-2\varepsilon}\left(\frac{p_{-1}^h}{2\varepsilon} + p_0^h\right), \tag{9}$$

so that the full result for the $O(\alpha_e^3)$ contribution to the QED pressure takes the form

$$p_3 = \frac{e^2 m_{\rm E}^4}{6(4\pi)^4}\left[\frac{p_{-1}^m + p_{-1}^h}{2\varepsilon} - p_{-1}^m \ln\left(\frac{m_{\rm E}}{\Lambda_{\rm h}}\right) - p_{-1}^h \ln\left(\frac{\mu}{\Lambda_{\rm h}}\right) + p_0^m + p_0^h\right]. \tag{10}$$

The technical details of the diagrammatic evaluation of the terms p_{-1}^m, p_{-1}^h, p_0^m and part of p_0^h are presented in the Supplemental Material [21]. In short, the computation starts from working out the analytic structure of the diagrams shown in Eqs. (5) and (7), after which their divergent contributions are separated from the finite parts. The divergent terms are evaluated fully analytically, and even though standard numerics must be used in the evaluation of the finite parts, these contributions can be obtained to nearly arbitrary precision.

The final result for the terms p_{-1}^m and p_0^m reads

$$\begin{aligned}\frac{p_{-1}^m}{N_f} &= 5 - \frac{66}{N_f} - \frac{\pi^2}{12}\left(7 - \frac{60}{N_f}\right) - 8\ln\left(\frac{\bar{\Lambda}}{2\mu}\right),\\ \frac{p_0^m}{N_f} &\approx (1-\ln 2)\left(5 - \frac{66}{N_f} - \frac{\pi^2}{12}\left(7 - \frac{60}{N_f}\right)\right)\\ &\quad + \left(13 - \frac{23\pi^2}{12} + \frac{20}{3}\ln 2 - \frac{32}{3}\ln^2 2 + 2\delta\right)\ln\left(\frac{\bar{\Lambda}}{2\mu}\right)\\ &\quad - 4\ln^2\left(\frac{\bar{\Lambda}}{2\mu}\right) + 1.05960 - \frac{1.03093}{N_f},\end{aligned} \tag{11}$$

while an explicit determination of the IR divergences of the hard diagrams, shown in detail in the Supplemental Material [21], verifies the expected result $p_{-1}^h = -p_{-1}^m$. This important fact verifies the full cancellation of $\Lambda_{\rm h}$ from the final expression for p_3 and also means that the two logarithms in Eq. (10) combine into the form $\ln(m_{\rm E}/\mu) \sim \ln(\alpha_e)/2$. The mixed sector is also confirmed to be gauge invariant on its own, akin to the observations made about the QCD soft sector in [14].

The remaining p_0^h term in Eq. (10) is associated to the finite parts of the 4-loop diagrams shown in Eqs. (6) and (7), and can, after proper renormalization, be shown to take the form

$$\frac{p_0^h}{N_f} = c_2 \ln^2\left(\frac{\bar{\Lambda}}{2\mu}\right) + c_1 \ln\left(\frac{\bar{\Lambda}}{2\mu}\right) + c_0. \tag{12}$$

Here, the coefficients c_1 and c_2 can be fully determined using the renormalization-scale invariance of the pressure and the known coefficients of the logarithmic terms in Eq. (11) (see the Supplemental Material [21]), giving $c_2 = 8/3$ and $c_1 = -275/9 - 31/(2N_f) + 13\pi^2/4 + 8/3\ln 2$. The last finite coefficient c_0 reads $c_0 = c_{0,0} + c_{0,1}/N_f + c_{0,2}/N_f^2$. The computation for the leading $c_{0,0}$ term [coming from the hard N_f^3-diagram in Eq. (7)] gives $c_{0,0} = 0.69328(3)$. The determination of the subleading parts $c_{0,1}$ and $c_{0,2}$, however, requires numerically demanding UV-divergent integrals and remains presently unknown.

TABLE I. List of numerical values for the coefficients $a_{3,1}$–$a_{3,6}$ appearing in Eq. (1), with δ being the same constant that appeared already in Eq. (1). For the definition of the coefficients $c_{0,1}$ and $c_{0,2}$, see Eq. (12).

$a_{3,1}$	0
$a_{3,2}$	$-\frac{5}{4} + \frac{33}{2}N_f^{-1} + \frac{1}{48}(7 - 60N_f^{-1})\pi^2$
$a_{3,3}$	2
$a_{3,4}$	$-\frac{2}{3}$
$a_{3,5}$	$-\frac{79}{9} + \frac{2}{3}\pi^2 + \frac{2}{3}(13 - 8\ln 2)\ln 2 + \delta - \frac{31}{4}N_f^{-1}$
$a_{3,6}$	$1.02270(2) + (2.70082 + \frac{1}{2}c_{0,1})N_f^{-1} + \frac{1}{2}c_{0,2}N_f^{-2}$

Collecting results from the above, the N^{3}LO pressure of cold and dense QED obtains the final form

$$p_3 = N_f p_{\rm LO}\left(\frac{\alpha_e}{\pi}\right)^3\left[-\frac{p_{-1}^m}{4}\ln\left(N_f\frac{\alpha_e}{\pi}\right) - \frac{p_{-1}^m}{2}\ln 2 + \frac{p_0^m + p_0^h}{2}\right], \tag{13}$$

where the parameter p_{-1}^m, determined entirely by the mixed diagrams, is seen to provide the coefficient of the only term nonanalytic in α_e, proportional to $(\alpha_e/\pi)^3\ln(N_f\alpha_e/\pi)$. Translating this result to the notation of Eq. (1), we then finally retrieve the main result of our paper in the form of a list of numerical values for the coefficients $a_{3,1}$–$a_{3,6}$, reproduced in Table I.

IV. RESULTS AND DISCUSSION

Inserting the newly determined coefficients into Eq. (1), we are now in a position to inspect the result for the pressure numerically and test its sensitivity with respect to the choice of the renormalization scale $\bar{\Lambda}$ and the value of the unknown coefficient c_0. In Fig. 1, we do exactly this by plotting the pressure evaluated at $\bar{\Lambda} = X\mu$ as a function of $\alpha_e(\bar{\Lambda} = 2\mu)$ and varying X by a factor of 2 around $X = 2$ in accordance with typical conventions in the field [14,30]. Concretely, in this figure, we take $N_f = 1$ and use the known three-loop running of α_e (see, e.g., [31]) to parametrize $\alpha_e(X\mu)$ in terms of $\alpha_e(2\mu)$, and then evaluate the pressure as a function of $\alpha_e(X\mu)$. The value of the unknown coefficient $c_{0,1} + c_{0,2}$ is finally varied within the range from -10 to 10, which appears as a natural choice given the magnitudes of the $O(\alpha_e^3)$ terms that have been determined. This range has also been seen to be in accordance with an analysis performed with the MiHO algorithm of Ref. [32].

In Fig. 1, we observe a dramatic decrease in the renormalization-scale sensitivity of the new N^{3}LO result in comparison to the previous order, which we believe to be at least partially due to the determination of all explicit

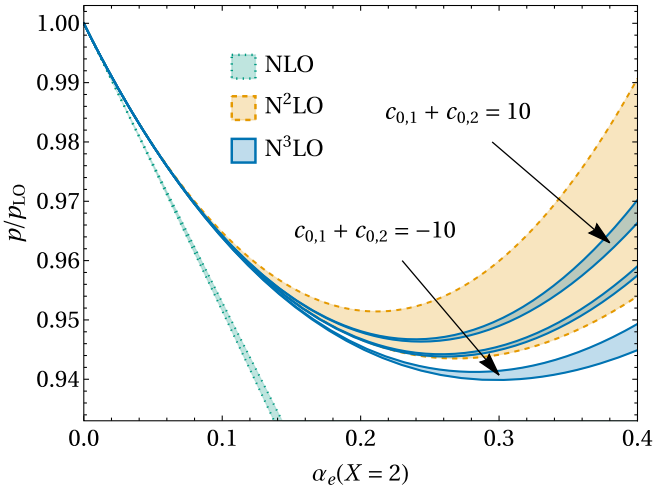

FIG. 1. The N^{3}LO pressure of cold and dense QED matter, displayed together with the old N^{2}LO and next-to-leading-order (NLO) results. Here, we have set $N_f = 1$, while allowing the sum $c_{0,1} + c_{0,2}$ of the yet-unknown constants to take values in $\{-10, 0, 10\}$. All bands have been obtained to varying the renormalization scale $\bar{\Lambda}$ by a factor of 2 around $\bar{\Lambda} = 2\mu$.

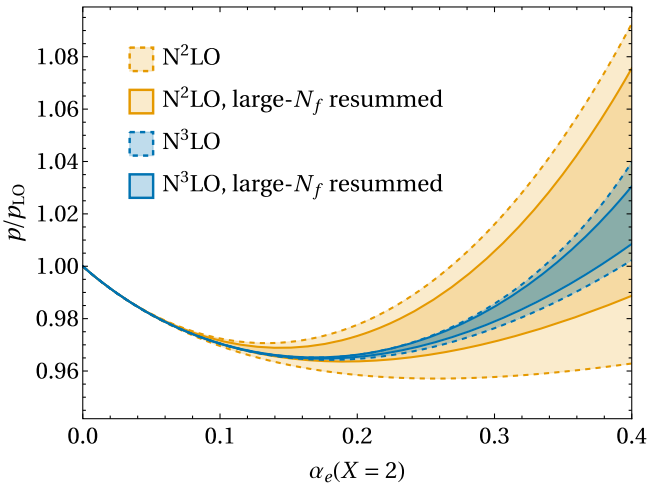

FIG. 2. The effect of the large-N_f resummation on the weak-coupling expansion of the pressure. Here, we have set $N_f = 3$ and $c_{0,1} = c_{0,2} = 3$.

logarithms at the $O(\alpha_e^3)$ level. At the same time, the result is clearly rather sensitive to the unknown hard $O(\alpha_e^3)$ contribution, which motivates vigorous future work towards completing the full N^{3}LO pressure calculation.

Next, we inspect the use of a resummation scheme motivated by the work of Moore, Ipp, and Rebhan [33–35], who determined the pressure of both QED and QCD in the limit of a large number of fermion flavors N_f, keeping the parameter $\alpha_e N_f$ finite. In the present context, where N_f is not large, this result can be used to resum all ring diagrams built using the full one-loop photon self-energy to infinite loop order. Just as with other resummation schemes, such as the widely-used hard thermal loop perturbation theory [36], this resummation amounts to including some higher-order terms in the weak-coupling expansion of the pressure, which is hoped to improve its convergence properties.

In Fig. 2, we demonstrate the effect of the large-N_f resummation for $N_f = 3$, displaying both the N^{2}LO and N^{3}LO pressures. As the figure clearly demonstrates, the resummation provides a marked improvement in the convergence of the result by taming some of the renormalization-scale dependence of the quantity, which motivates its eventual use also in the context of dense QCD. We also note in passing (see the Supplemental Material [21]) that our new calculation provides the coefficients 3.18(5) and 3.4(3) in Eq. (3.14) of [35] to the much improved precision of $(60 - 7\pi^2 + 96\ln 2)/18 \approx 3.1919388$ and 3.36388(4), respectively.

Finally, let us briefly study the behavior of the speed of sound c_s in cold and dense QED matter. This quantity is particularly interesting in QCD, as there is strong tension between the common expectation that it rises close to the speed of light in dense nuclear matter and the fact that at high temperatures, it is known to approach the asymptotic conformal value of $c_s^2 = 1/3$ from below. In QED, the conformal limit is known to be broken as the sign of the beta function indicates that the leading correction to the noninteracting massless limit comes with a positive sign. This is indeed verified by our result, shown in Fig. 3. We, however, observe that the higher-order corrections prevent the speed of sound from significantly exceeding the conformal value. Lastly, we note the extremely good convergence of this quantity even at very large couplings.

In summary, we have found that at least in the case of cold and dense QED matter, including contributions beyond N^{2}LO has a notable effect on the convergence

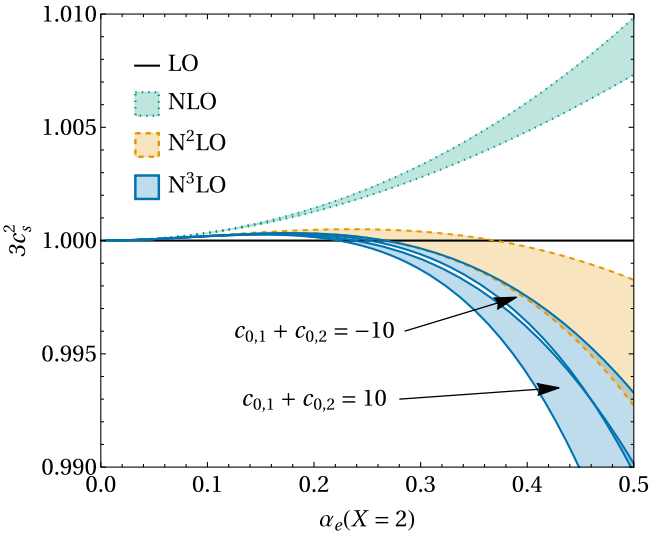

FIG. 3. The speed of sound squared (times three) for different orders of the weak-coupling expansion. Here, we have again set $N_f = 1$.

properties of the pressure. This provides compelling reasons to pursue the evaluation of further N^3LO terms of the pressure of cold and dense matter. With the coefficients $c_{0,1}$ and $c_{0,2}$ fixed, our results demonstrate that the renormalization-scale uncertainty of the pressure will drop to a small fraction of the previous N^2LO result at all coupling values of relevance for even QCD. This implies that there is good reason to believe that performing similar improvements within QCD will allow the perturbative EOS of dense quark matter to become applicable at substantially lower densities than what has been possible so far. This would have dramatic effects for the model-independent determination of the neutron-star-matter EOS as highlighted by past interpolation works [37–39] and the more recent results that enable rigorously translating perturbative constraints to lower densities using standard thermodynamic relations [40,41]. We underline that the weak-coupling computations presented in this work, once generalized to QCD, would not be sensitive to any color-superconducting phases, since only gluons with nonperturbatively small energies $\sim \exp(-\#/\sqrt{\alpha})$ receive corrections to their screening from quark Cooper pairing [42,43].

Finally, let us briefly comment on the generalizations necessary to complete the present calculation in QCD. While it is true that there exists an additional soft NLO correction to the gluon self-energy in QCD, the corresponding contribution to the zero-temperature pressure has already been determined in [13,14]. Hence, again at zero temperature, the only contribution missing in the mixed sector is the two-loop HTL gluon self-energy. Thanks to the new technical advances made in the QED case here and in the companion paper [24], this QCD contribution is straightforward (if tedious) to compute. In order to complete the computation of hard sector, the only remaining terms needed are the currently unknown coefficients $c_{0,1}$ and $c_{0,2}$, extended to QCD. On a technical level, the computation of these coefficients (both in QED and QCD) involves complicated UV-sensitive 4-loop diagrams, which require novel methods in finite-density multiloop computations, e.g., see Refs. [44,45].

ACKNOWLEDGMENTS

The authors would like to thank Andreas Ipp, Niko Jokela, and Aleksas Mazeliauskas for useful discussions. T. G. has been supported in part by the Deutsche Forschungsgemeinschaft (DFG, German Research Foundation)—Project-ID 279384907—SFB 1245 and by the State of Hesse within the Research Cluster ELEMENTS (Project ID 500/10.006). J. Ö., R. P., P. S., K. S., and A. V. have been supported by the Academy of Finland Grants No. 1322507 and No. 347499 as well as by the European Research Council, Grant No. 725369. In addition, K. S. gratefully acknowledges support from the Finnish Cultural Foundation, and J.Ö. from the Vilho, Yrjö and Kalle Väisälä Foundation of the Finnish Academy of Science and Letters (FundRef ID http://dx.doi.org/10.13039/501100016032).

[1] K. M. O'Hara, S. L. Hemmer, M. E. Gehm, S. R. Granade, and J. E. Thomas, Science **298**, 2179 (2002).
[2] S. A. Hartnoll, A. Lucas, and S. Sachdev, arXiv:1612.07324.
[3] S. Kobayashi, D. Mateos, S. Matsuura, R. C. Myers, and R. M. Thomson, J. High Energy Phys. 02 (2007) 016.
[4] A. F. Faedo, A. Kundu, D. Mateos, and J. Tarrio, J. High Energy Phys. 02 (2015) 010.
[5] S. Chandrasekhar, Astrophys. J. **74**, 81 (1931).
[6] J. M. Lattimer and M. Prakash, Science **304**, 536 (2004).
[7] J. Ghiglieri, A. Kurkela, M. Strickland, and A. Vuorinen, Phys. Rep. **880**, 1 (2020).
[8] B. A. Freedman and L. D. McLerran, Phys. Rev. D **16**, 1130 (1977).
[9] B. A. Freedman and L. D. McLerran, Phys. Rev. D **16**, 1147 (1977).
[10] B. A. Freedman and L. D. McLerran, Phys. Rev. D **16**, 1169 (1977).
[11] A. Kurkela and A. Vuorinen, Phys. Rev. Lett. **117**, 042501 (2016).
[12] T. Gorda, A. Kurkela, P. Romatschke, S. Säppi, and A. Vuorinen, Phys. Rev. Lett. **121**, 202701 (2018).
[13] T. Gorda, A. Kurkela, R. Paatelainen, S. Säppi, and A. Vuorinen, Phys. Rev. Lett. **127**, 162003 (2021).
[14] T. Gorda, A. Kurkela, R. Paatelainen, S. Säppi, and A. Vuorinen, Phys. Rev. D **104**, 074015 (2021).
[15] T. Gorda and S. Säppi, Phys. Rev. D **105**, 114005 (2022).
[16] L. Fernandez and J.-L. Kneur, Phys. Rev. Lett. **129**, 212001 (2022).
[17] V. Baluni, Phys. Rev. D **17**, 2092 (1978).
[18] C. Coriano and R. R. Parwani, Phys. Rev. Lett. **73**, 2398 (1994).
[19] R. R. Parwani and C. Coriano, Nucl. Phys. **B434**, 56 (1995).
[20] A. Vuorinen, Phys. Rev. D **68**, 054017 (2003).
[21] See Supplemental Material at http://link.aps.org/supplemental/10.1103/PhysRevD.107.L031501 for technical details of the perturbative computation of the pressure, the $O(N_f{}^3)$ diagram, and the renormalization of the result, which includes Refs. [22,23].
[22] A. Gynther, A. Kurkela, and A. Vuorinen, Phys. Rev. D **80**, 096002 (2009).
[23] W. E. Caswell, Phys. Rev. Lett. **33**, 244 (1974).

[24] T. Gorda, A. Kurkela, J. Österman, R. Paatelainen, S. Säppi, P. Schicho, K. Seppänen, and A. Vuorinen, companion paper, Phys. Rev. D **107**, 036012 (2023).
[25] C. Manuel, J. Soto, and S. Stetina, Phys. Rev. D **94**, 025017 (2016); **96**, 129901(E) (2017).
[26] S. Carignano, C. Manuel, and J. Soto, Phys. Lett. B **780**, 308 (2018).
[27] S. Carignano, M. E. Carrington, and J. Soto, Phys. Lett. B **801**, 135193 (2020).
[28] E. Braaten and R. D. Pisarski, Nucl. Phys. **B337**, 569 (1990).
[29] M. Le Bellac, *Thermal Field Theory*, Cambridge Monographs on Mathematical Physics (Cambridge University Press, Cambridge, England, 2011).
[30] A. Kurkela, P. Romatschke, and A. Vuorinen, Phys. Rev. D **81**, 105021 (2010).
[31] P. A. Baikov, K. G. Chetyrkin, J. H. Kuhn, and J. Rittinger, J. High Energy Phys. 07 (2012) 017.
[32] C. Duhr, A. Huss, A. Mazeliauskas, and R. Szafron, J. High Energy Phys. 09 (2021) 122.
[33] G. D. Moore, J. High Energy Phys. 10 (2002) 055.
[34] A. Ipp, G. D. Moore, and A. Rebhan, J. High Energy Phys. 01 (2003) 037.
[35] A. Ipp and A. Rebhan, J. High Energy Phys. 06 (2003) 032.
[36] N. Su, Commun. Theor. Phys. **57**, 409 (2012).
[37] E. Annala, T. Gorda, A. Kurkela, and A. Vuorinen, Phys. Rev. Lett. **120**, 172703 (2018).
[38] E. Annala, T. Gorda, A. Kurkela, J. Nättilä, and A. Vuorinen, Nat. Phys. **16**, 907 (2020).
[39] E. Annala, T. Gorda, E. Katerini, A. Kurkela, J. Nättilä, V. Paschalidis, and A. Vuorinen, Phys. Rev. X **12**, 011058 (2022).
[40] O. Komoltsev and A. Kurkela, Phys. Rev. Lett. **128**, 202701 (2022).
[41] T. Gorda, O. Komoltsev, and A. Kurkela, arXiv:2204.11877.
[42] H. Malekzadeh and D. H. Rischke, Phys. Rev. D **73**, 114006 (2006).
[43] M. G. Alford, A. Schmitt, K. Rajagopal, and T. Schäfer, Rev. Mod. Phys. **80**, 1455 (2008).
[44] I. Ghisoiu, T. Gorda, A. Kurkela, P. Romatschke, M. Säppi, and A. Vuorinen, Nucl. Phys. **B915**, 102 (2017).
[45] T. Gorda, J. Österman, and S. Säppi, Phys. Rev. D **106**, 105026 (2022).